Reactive quenching of OH($A\ ^2\Sigma^+$) by D_2 studied using crossed molecular beams

Mariví Ortiz-Suárez, Mark F. Witinski, and H. Floyd Davis[a)]
Department of Chemistry and Chemical Biology, Baker Laboratory, Cornell University, Ithaca, NY 14853-1301

(Received 13 March 2006; accepted 28 April 2006; published online 22 May 2006)

Reactive quenching of OH($A\ ^2\Sigma^+, v=0$) by D_2 forming HOD+D was studied in crossed molecular beams. The D atom products are primarily forward scattered relative to the incident D_2. The dominant mechanism involves a direct reaction from relatively large impact parameters with ~88% of the available energy appearing in HOD internal excitation. © *2006 American Institute of Physics*. [DOI: 10.1063/1.2206779]

I. INTRODUCTION

It has been known for many years that electronically excited hydroxyl radicals are rapidly quenched by collisions with small molecules.[1–3] The OH($A\ ^2\Sigma^+$) quenching rate constants for many different atomic and molecular partners have been measured as a function of temperature.[1] In most studies, the quenching was monitored through the disappearance of OH($A\ ^2\Sigma^+$), the products resulting from the quenching events were not identified. For quenching of OH($A\ ^2\Sigma^+$) by molecules containing hydrogen (RH), both physical quenching forming OH($X\ ^2\Pi$)+RH, as well as bimolecular reaction forming H_2O+R, are possible[4–6] The simplest, and most-studied molecular quenchers of OH($A\ ^2\Sigma^+$) are H_2 and D_2. The total quenching rate constant is nearly gas kinetic, suggesting that attractive interactions play an important role.[1–3] The bimolecular reaction forming H_2O (or HOD) is exothermic by 451 kJ/mol, and is thought to proceed without any potential energy barrier along the reaction pathway.[4–10] Reaction could therefore represent a significant fraction of quenching events.[6–10]

The OH($A\ ^2\Sigma^+$)+H_2(D_2) reaction has become a benchmark system for examining nonadiabatic quenching processes. The crossing regions between the ground state and excited state potential energy surfaces for OH($A\ ^2\Sigma^+$)+H_2(D_2) lead to conical intersections.[4–10] Lester's group has carried out extensive studies of photoinitiated processes within van der Waals complexes involving OH.[11,12] They have also studied quenching reactions initiated by bimolecular collisions.[4–6] In these studies, a beam containing nitric acid (HNO_3) was co-expanded with the molecular reactant and photolyzed at 193 nm near the nozzle orifice, producing OH+NO_2. The OH radicals were excited to the $A\ ^2\Sigma^+$ state slightly further downstream, in the region where collisions were still occurring. The H or D atom products from bimolecular reactions of OH($A\ ^2\Sigma^+$)+D_2 were excited to the $2p$ state by 2-photon excitation at 243 nm, and the VUV fluorescence intensity monitored. By scanning the UV probe laser wavelength, Doppler spectra of the nascent H or D atoms were recorded. The D atom translational energy release was bimodal, with the dominant pathway involving formation of water with a high degree of vibrational excitation. A second minor pathway led to a larger D atom kinetic release, implying that the HOD counter-fragment was vibrationally colder.

We have studied the quenching reaction using crossed molecular beams, employing the Rydberg time-of-flight method.[13] While the large amount of available energy in OH($A\ ^2\Sigma^+$)+D_2 renders the determination of HOD vibrational branching ratios unlikely, a measurement of the product angular distribution and translational energy release should provide new insight into the reaction dynamics.

II. EXPERIMENTAL

These experiments were carried out using a fixed source, rotatable detector crossed molecular beams apparatus.[14] The OH beam was produced by 193 nm photodissociation of anhydrous nitric acid (0 °C) seeded in a pulsed supersonic expansion of hydrogen at 2 atm. The velocity of the OH beam was ~2350 m/s and its rotational temperature (characterized using laser-induced fluorescence spectroscopy) was approximately 85 K. A pulsed supersonic expansion of pure D_2 (1.3 atm) with a beam velocity of 2000 m/s leads to a mean collision energy of 15.5 kJ/mol.

Each beam was generated in separately pumped chambers and collimated by nickel skimmers before crossing at a fixed 90° angle, 8.0 cm away from each pulsed valve. Due to the relatively short fluorescence lifetime of OH($A\ ^2\Sigma^+$),[15] excitation from the ground state was carried out in the beam crossing region by a Nd:YAG (Spectra-Physics Lab 170-30) pumped dye laser (Lambda Physik FL3002) using the $Q_1(l)N'=1$, $J'=3/2$ transition in the (0,0) vibronic band near 308 nm.

After a short delay time (20 ns), D atom products were excited in the interaction region to high-n Rydberg levels using a two-photon excitation scheme employing lasers introduced perpendicular to the plane of the molecular beams. The first photon, near 121 nm, was produced by resonance enhanced four-wave mixing of two laser beams, at 212 nm and 846 nm, in a gas cell containing a 3.5:1 mixture of

a)Corresponding author. Electronic mail: hfd1@cornell.edu

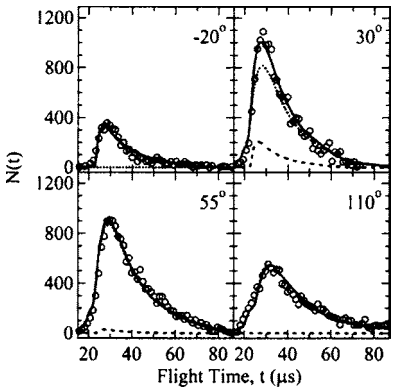

FIG. 1. D atom time-of-flight spectra at four laboratory angles (circles) with overall fits (solid line). Laboratory angles are measured relative to the OH beam ($\Theta=0^{\circ}$). The dominant ($\sim$87%) forward scattered channel (channel 1) is denoted by a dotted line, and the minor ($\sim$13%) backward scattered channel (channel 2) is denoted by a dashed line.

Ar:Kr.[16] Excitation to $n=40$ was accomplished using the doubled output of a third dye laser operating near 365 nm.

The "tagged" D atoms flew 33.3 cm through a field-free region before being field ionized ((–2.3 kV/cm) in the region between a grounded mesh and a microchannel plate (MCP), where the ions were collected. Under our current experimental arrangement, we have access to an angular range of 140° in the laboratory frame. In addition to taking TOFs at intervals throughout this range under the conditions described above, a considerable amount of data was recorded in which the OH excitation laser was detuned slightly from the *A*-state resonance. These scans, which led to only very small signal, were subtracted from the signal obtained with the laser tuned to the OH absorption maximum.

III. RESULTS

The time-of-flight (TOF) spectra for D atoms from the title reaction are shown in Fig. 1. The integrated laboratory angular distribution is shown in Fig. 2. The laboratory angles are given with respect to the OH beam ($\Theta=0^{\circ}$); the D_2 beam is at $\Theta=90^{\circ}$. The solid-line fits were obtained using a forward convolution program which takes as input a center-of-mass translational energy, $[P(E)]$, and angular distribution,

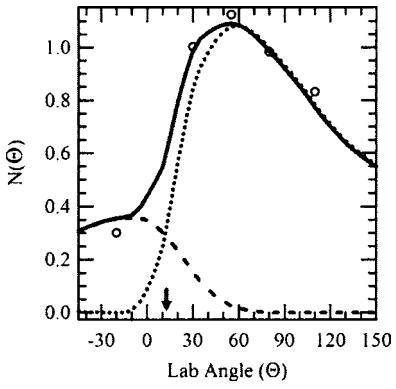

FIG. 2. Integrated D atom laboratory angular distribution (circles) with overall fits (solid line). Contributions from channel 1 (dotted line) and channel 2 (dashed line) are indicated. The angle of the CM of the system ($\Theta=12^{\circ}$) is marked with an arrow.

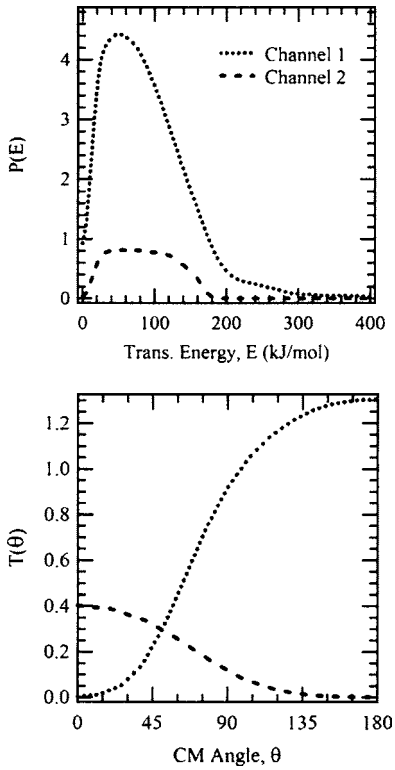

FIG. 3. Top panel: D atom center-of-mass translational energy distributions. Bottom panel: Center-of-mass angular distributions, $T(\theta)$. Contributions from channel 1 (dotted line) and channel 2 (dashed line) are indicated.

$[T(\theta)]$, and averages over the known experimental parameters to generate simulated data. The trial translational energy and angular distributions were iteratively improved until the simulations matched the experimental data, both in shape and in integrated area as a function of laboratory angle.

We initially attempted to simulate the experimental data using a single uncoupled translational energy distribution, $P(E)$, and center-of-mass (CM) angular distribution, $T(\theta)$. The laboratory angular distribution indicates that the CM angular distribution is highly anisotropic, with the product D atoms preferentially scattered "forward" relative to the incident D_2 molecules. We were able to obtain reasonable agreement between our simulation and the measured laboratory angular distribution using a single $P(E)$ and $T(\theta)$. However, the simulations of the TOF data were not able to correctly model the fastest contribution of D atoms at each laboratory angle. Specifically, a $P(E)$ able to properly simulate the TOF data at large scattering angles (e.g., 110°) would substantially overestimate the highest energy contribution at smaller laboratory angles. This implies that the maximum D atom translational energy release in the forward direction (relative to D_2) is somewhat greater than in the backward direction.

We therefore employed a second, more flexible functional form using two $P(E)$ and $T(\theta)$ distributions, i.e., $P_1(E)T_1(\theta)+P_2(E)T_2(\theta)$. This approach is common in cases where the overall reaction involves more than one mechanism. In the present case, subscripts 1 and 2 are assigned to the two dynamically distinct reaction pathways. As shown in Fig. 3, the dominant ($\sim$87%) contribution, channel 1, de-

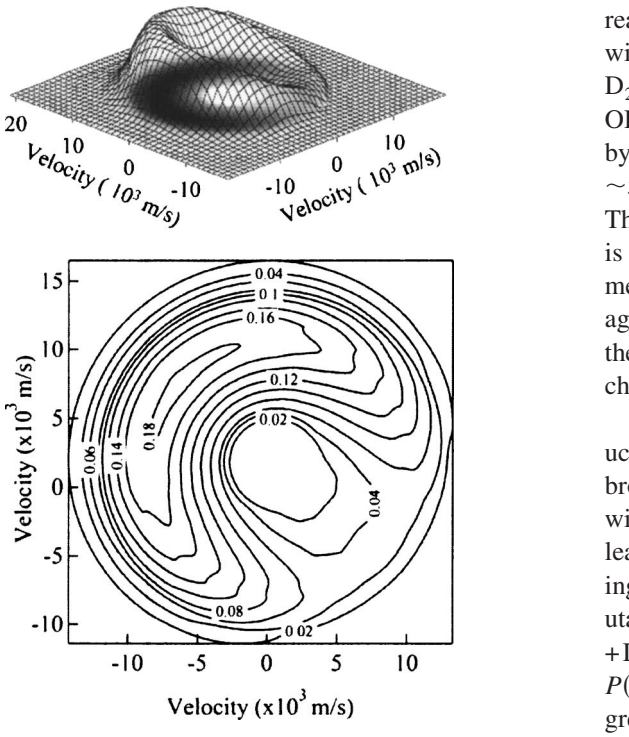

FIG. 4. Overall center of mass product flux contour map for D atom products from $OH(A\ ^2\Sigma^+)+D_2 \rightarrow HOD+D$.

noted by a dotted line, involves a forward scattered D atom channel with a broad translational energy release. The second, minor (~13%) channel (channel 2), denoted by a dashed line, incorporated a backward scattered angular distribution. The translational energy release distributions for the two channels are similar. However, the maximum translational energy release for channel 2 does not extend to as high values as in channel 1. The optimized distributions used to produce the solid line fits in Figs. 1 and 2 are shown in Fig. 3. The overall D atom product flux contour map is shown in Fig. 4.

It is also possible to simulate the data using a forward and a forward-backward scattered angular distribution. In this case, the contribution from the dominant forward scattered channel is ~75%, and the forward-backward scattered channel is ~25%. Since the $P(E)$ distributions are not very different for the two channels, the product flux contour map derived from this $P(E)/T(\theta)$ combination is essentially the same as that shown in Fig. 4.

IV. DISCUSSION

The product flux contour map (Fig. 4) indicates that the D atom products are preferentially forward scattered relative to the incident D_2 molecules. This implies that the dominant reaction mechanism is direct, occurring on timescales shorter than that for rotation of the OH-D_2 pair, i.e., on subpicosecond timescales. The preferential forward scattering is a signature of a mechanism in which the incoming $OH(A\ ^2\Sigma^+)$ reactant picks up a D atom from D_2 at relatively large impact parameters, with the newly-formed HOD continuing in nearly the same direction as the incident $OH(A\ ^2\Sigma^+)$. This behavior is exactly the opposite to that for the ground state reaction, which involves small impact parameter collisions with the D atoms backward scattered relative to the incident D_2 molecules (i.e., HOD is backward scattered relative to OH).[14,17] The $OH(A\ ^2\Sigma^+, v=0)+D_2 \rightarrow HOD+D$ is exoergic by451 kJ/mol. The translational energy distribution peaks at ~55 kJ/mol, but includes contributions up to ~340 kJ/mol. Thus, the most probable internal energy of the HOD product is ~410 kJ/mol, which at the collision energy of this experiment corresponds to ~88% of the total available energy. In agreement with previous findings,[4,6] a significant fraction of the available energy, largely $OH(A\ ^2\Sigma^+)$ electronic energy, is channeled into HOD vibrational excitation.

The kinetic energy release distribution for D atom products scattered at wider CM angles (channel 2) is also very broad. A possible physical origin for D atom scattering at wide CM angles involves small impact parameter collisions, leading to direct rebound dynamics.[18] The direct backscattering seen in the $OH(X\ ^2\Pi_i)+D_2 \rightarrow HOD+D$ reaction is attributable to this mechanism.[14,17] For channel 2 in $OH(A\ ^2\Sigma^+)+D_2$, the highest translational energy contribution to the $P(E)$ (observed in channel 1) is apparently absent. Thus, a greater fraction of available energy is deposited into HOD vibrational excitation for small impact parameter reactive collisions.

An alternative source of wide-angle scattering could involve formation of HOD_2 complexes with lifetimes comparable to or longer than their rotational periods.[19] The quenching reaction $OH(A\ ^2\Sigma^+)+D_2 \rightarrow H+D_2O$ has been observed,[6] suggesting that HOD_2 complexes are formed to some extent during the reaction. However, the nature of the HOD_2 intermediate(s) in this reaction, particularly their lifetimes, remains uncertain. It is well-known that conical intersections are formed from the crossings of the potential energy surfaces correlating to $OH(A\ ^2\Sigma^+)+D_2$ and $OH(X\ ^2\Pi_i)+D_2$.[7–10] Conical intersections funnel the $OH(A\ ^2\Sigma^+)+D_2$ reactant flux towards the ground state $OH(X\ ^2\Pi_i)+D_2$ quenching products, and also to HOD+D or D_2O+H reaction products. The earliest calculations addressing the formation of water resulting from the quenching of $OH(A\ ^2\Sigma^+)$ by H_2 concluded that approach in C_{2v} symmetry, with the H atom in OH pointing away from the H_2, leads to a conical intersection.[7] Passage through this region was expected to proceed with no significant potential energy barrier. Subsequently, more detailed calculations by Yarkony,[8] and by Hoffman and Yarkony,[9] have located the seams of conical intersections in C_{2v}, $C_{\infty v}$, and C_s symmetries. Detailed analysis of the regions near these seams have provided the first theoretical insight into the pathways leading to H_2O+H or to quenching yielding $OH(X\ ^2\Pi_i)+H_2$.[8,9] The reacting system may proceed directly through the conical intersection region, leading to "direct" product formation.[4,6] Alternatively, reactants might become trapped in the upper attractive adiabatic well formed by the avoided crossing of diabatic curves, effectively increasing the timescale for reaction.[4,6] It has been suggested that this trapping mechanism might provide a mechanism for energy randomization within the complex prior to formation of chemical products.[4,6] Our finding that the wide-angle scat-

tered D atom products are formed with slightly smaller maximum translational energy release (with slightly larger average HOD vibrational energy) than the dominant channel might be taken as evidence for partial energy randomization. It is believed that the conical intersections lie at energies approximately 1 eV below that of the separated $OH(A\ ^2\Sigma^+)+D_2$ reactants, which is more than 3 eV above the HOD +D product. Whether or not the wide-angle scattered HOD +D products might result from such trapping, which would imply lifetimes on the order of a rotational period, remains an open question. It would appear that trajectory calculations might provide important insight into the question of complex lifetimes and energy disposal following passage through this region of the potential energy surface.

We hope that these initial results stimulate new theoretical work on this system. Further experiments currently underway in our laboratory include studies of the quenching of $OH(A\ ^2\Sigma^+, v=1)$.

ACKNOWLEDGMENT

This research was supported by the office of Science, U.S. Department of Energy under Grant No. DE-FG02-00ER15095. The authors acknowledge valuable discussions with Professor M. I. Lester.

[1] B. L. Hemming and D. Crosley, J. Phys. Chem. A **106**, 8992 (2002).
[2] B. Hemming, D. R. Crosley, J. E. Harrington, and V. Sick, J. Chem. Phys. **115**, 3099 (2001).
[3] D. R. Crosley, J. Phys. Chem. **93**, 6273 (1989).
[4] D. T. Anderson, M. W. Todd, and M. I. Lester, J. Chem. Phys. **110**, 11117 (1999).
[5] I. B. Pollack, Y. X. Lei, T. A. Stephenson, and M. I. Lester, Chem. Phys. Lett. **421**, 324 (2006).
[6] M. W. Todd, D. T. Anderson, and M. I. Lester, J. Phys. Chem. A **105**, 10031 (2001).
[7] M. I. Lester, R. A. Loomis, R. L. Schwartz, and S. P. Walch, J. Phys. Chem. A **101**, 9195 (1997).
[8] D. R. Yarkony, J. Chem. Phys. **111**, 6661 (1999).
[9] B. C. Hoffmann and D. R. Yarkony, J. Chem. Phys. **113**, 10091 (2000).
[10] D. R. Yarkony, J. Phys. Chem. **100**, 18612 (1996).
[11] R. A. Loomis and M. I. Lester, Annu. Rev. Phys. Chem. **48**, 643 (1997).
[12] M. D. Wheeler, D. T. Anderson, and M. I. Lester, Int. Rev. Phys. Chem. **19**, 501 (2000).
[13] L. Schnieder, W. Meier, K. H. Welge, M. N. R. Ashfold, and C. M. Western, J. Chem. Phys. **92**, 7027 (1990).
[14] B. Strazisar, C. Lin, and H. F. Davis, Science **290**, 958 (2000).
[15] R. A. Sutherland and R. A. Anderson, J. Chem. Phys. **58**, 1226 (1973).
[16] J. P. Marangos, N. Shen, H. Ma, M. H. R. Hutchinson, and J. P. Connerade, J. Opt. Soc. Am. B **7**, 1254 (1990).
[17] M. Alagia, N. Balucani, P. Casavecchia, D. Stranges, G. G. Volpi, D. C. Clary, A. Kliesch, and H.-J. Werner, Chem. Phys. **207**, 389 (1996).
[18] See, for example, the discussion of the angular distributions for the reactions $F+H_2$ and $K+CH_3I$, both of which lead to rebound dynamics, in R. D. Levine, and R. B. Bernstein, *Molecular Reaction Dynamics and Chemical Reactivity* (Oxford University Press, New York, 1987).
[19] W. B. Millers, S. A. Safron, and D. R. Herschbach, Discuss. Faraday Soc. **44**, 108 (1967); J. Chem. Phys. **56**, 3581 (1972).